ISSN 0036-0244, Russian Journal of Physical Chemistry A, 2013, Vol. 87, No. 11, pp. 1881–1887. © Pleiades Publishing, Ltd., 2013.
Original Russian Text © S.N. Lanin, A.A. Bannykh, N.V. Kovaleva, 2013, published in Zhurnal Fizicheskoi Khimii, 2013, Vol. 87, No. 11, pp. 1910–1916.

PHYSICAL CHEMISTRY OF SURFACE PHENOMENA

Adsorption Properties of Alumina Modified with Nickel Nanoparticles

S. N. Lanin, A. A. Bannykh, and N. V. Kovaleva

Department of Chemistry, Moscow State University, Moscow, 119991 Russia

e-mail: SNLanin@phys.chem.msu.ru

Received December 26, 2012

Abstract—Adsorption properties of parent γ-alumina, and γ-alumina, modified with nickel nanoparticles (from 0.6 to 18 wt %), are investigated by dynamic sorption. *N*-hexane, benzene, chloroform, diethyl ether, chlorobenzene, and *o*-dichlorobenzene are used as test adsorbates. Adsorption isotherms are measured, and isosteric adsorption heats are calculated. Electron-donating and electron-accepting characteristics of surfaces of parent γ-alumina and γ-alumina, modified with Ni nanoparticles, are estimated. It is established that the surface of parent γ-alumina has mainly electron-accepting properties, while the surface of γ-alumina modified with Ni nanoparticles has electron-donating properties. It is shown that benzene and chlorobenzene are sorbed via physical adsorption on the parent and modified γ-alumina, and *o*-dichlorobenzene is sorbed via chemosorption.

Keywords: alumina, modification with nickel nanoparticles, dynamic sorption.

DOI: 10.1134/S0036024413100129

INTRODUCTION

In recent years, systems of metal nanoparticles have been intensively investigated due to their properties, which differ from those of bulk metals. Such systems are of interest because the transition to the nanometer range of particles is accompanied in a number of cases by a sharp rise in the metal's catalytic activity [1–5]. In order to understand the mechanisms of catalytic reactions that proceed on immobilized metal nanoparticles, information on the strength and nature of these particles' interactions with reagents and the support's surface is required.

In this work, the adsorption properties of parent γ-alumina (which is widely used in supports for heterogeneous catalysts of different processes), and γ-alumina modified with nickel nanoparticles, which is used as a catalyst particularly in reactions of hydrodechlorination [6] and hydration, including a large group of hydrogen bonding reactions via the unsaturated bonds in nonsaturated and aromatic hydrocarbons [7].

EXPERIMENTAL

Adsorbents

γ-Alumina (Sigma-Adrich) with a specific surface area of 110 m^2/g, a pore volume of 0.29 cm^3/g, and a pore diameter of 340 Å was used as the support adsorbent. Nanocomposites of Ni/γ-alumina with Ni contents of 0.6, 1.5, 3, 12, and 18 wt %, were prepared by treating γ-alumina in a solution of nickel nitrate hexahydrate, followed by heating in air at 550°C for three hours and reduction in a hydrogen flow (12 cm^3/min) at 450°C. Alumina prepared by treatment in nitric acid solution (without use of nickel nitrate) and then heated in air at 550°C for three hours and reduced in a hydrogen flow (12 cm^3/min) at 450°C was also used, along with parent γ-$Al_2O_3^*$ as a reference adsorbent.

Nanocomposite samples were studied by X-ray diffraction on a Rigaku D/MAX 2500 rotating anode diffractometer (Japan). The mean diameter (D_{hkl}) of the Ni nanoparticles was estimated using the Debye-Scherrer formula,

$$D_{hkl} = k\lambda/\beta_{hkl}\cos\theta_{hkl}, \quad (1)$$

where $k = 0.89$; λ is wavelength, Å; θ_{hkl} is the angle of diffraction; and β_{hkl} is the half-width of diffraction peak in radians.

Adsorbates

Chlorobenzene and *o*-dichlorobenzene were used as reagent adsorbates. *n*-Alkanes (C_6–C_8), which have only nonspecific (dispersive) interactions with the surface of any adsorbent, and benzene, chloroform, and diethyl ether, which can have specific (donor-acceptor) interactions with functional groups of an adsorbent surface, were used to investigate the texture and chemistry of surface of γ-alumina and Ni/γ-alumina nanocomposites. Characteristics of these reagents are given in Table 1.

Table 1. Characteristic of test adsorbates (*M* is molecular mass, μ is the dipole moment, α is the total polarizing ability of molecule, and *AN* and *DN* are the electron-accepting and electron-donating energy characteristics of the molecules [8])

Adsorbate	*M*	μ, D	α, Å^3	*DN*, kJ/mol	*AN*
C_6H_5Cl	112.6	1.72		–	–
$C_6H_4Cl_2$	147	2.24		–	–
n-C_6H_{14}	86.17	0	11.9	0	0
n-C_7H_{16}	100.2	0	13.7	0	0
n-C_8H_{18}	114.2	0	15.6	0	0
C_6H_6	78	0	10.4	0.4	8.2
$CHCl_3$	119.4	1.15	8.2	0	23
$(C_2H_5)_2O$	79.1	1.70	9.0	80.3	3.9

Table 2. Size of Ni nanoparticles (*d*, nm) of Ni/Al_2O_3 nanocomposite surfaces

Composite	*d*
6% Ni/ γ-Al_2O_3	4.7
12% Ni/ γ-Al_2O_3	5.3
18% Ni/ γ-Al_2O_3	20.4

Gas-Chromatography Studies

Adsorption properties were studied via dynamic sorption on a Crystallux-4000M chromatograph equipped with thermal conductivity detector. Glass columns 20 cm long and with inner diameters of 2 mm were used for the physicochemical measurements. Helium was used as the carrier gas at a flow rate of 25–30 mL/min. Prior to measurements, the adsorbent was treated in a carrier-gas flow in a chromatograph column at 200°C for 8 h. The volume of injected adsorbate specimens was varied from 0.5 to 5 μL.

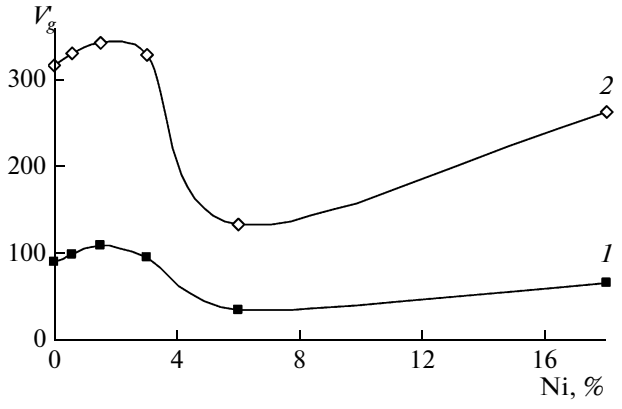

Fig. 1. Dependences of specific retention volumes (V_g', mL/g) on Ni content in Ni/Al_2O_3 nanocomposites: (*1*) chlorobenzene; (*2*) *o*-dichlorobenzene.

Specific retention volumes were measured for C_6H_5Cl and $C_6H_4Cl_2$ in the temperature range of 125–150°C and for *n*-C_6H_{14}, C_6H_6, $CHCl_3$, and $(C_2H_5)_2O$ in the temperature range of 100–110°C in the area of low surface filling; adsorption isotherms and isosteric heats of adsorption were calculated using the technique described in [9].

Monolayer Volume

The volume of Ni nanoparticle monolayers on a γ-alumina surface was estimated from the dependency of specific retention volumes (V_m) of C_6H_5Cl and $C_6H_4Cl_2$ on the nickel content of nanocomposites (Fig. 1). A well-defined inflection is observed in such dependences in the monolayer area [10]. As can be seen from Fig. 1, the monolayer volume corresponds to a nickel content of 6 wt % or 0.55 mg/m^2. On γ-alumina samples with nickel contents of more than 6%, adsorption apparently occurs on Ni nanoclusters.

RESULTS AND DISCUSSION

Size and Content of Nanoparticles

The Ni phase is not observed when studying nanocomposites with Ni contents of less than 6% via X-ray diffraction. Phases of both Ni (Ni type) and nickel oxide NiO (NaCl type) are detected in composites of 6% Ni/γ-alumina and 12% Ni/γ-Al_2O_3 composition. Theoretical diffraction patterns were constructed for the Ni and NiO phases (Fig. 2). In studying composites of 18% Ni/γ-alumina composition, it was established that it contains Ni (Ni type) and NiO (NaCl type) phases, with the Ni phase predominating considerably. The mean diameters of nickel nanoparticles are presented in Table 2.

Adsorption Isotherms of Test Adsorbates

Adsorption isotherms of test adsorbates on $Al_2O_3^*$, 12% Ni/γ-Al_2O_3, and 18% Ni/γ-Al_2O_3 are presented in Fig. 3 as examples. Specific surface areas (*s*, m^2/g) were calculated via BET method from adsorption isotherms of *n*-hexane at 100°C. The parameters of porous structures were estimated using the Dubinin–Radushkevich equation [11]. The radii of macropores (*r*) were calculated from the dependency of the characteristic adsorption energy (E_0) [12],

$$r = 12/E_0. \quad (2)$$

Results from our calculations are presents in Table 3.

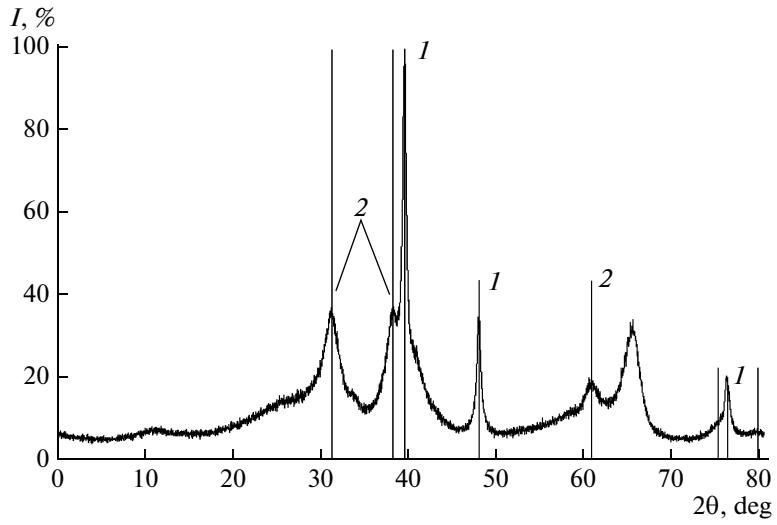

Fig. 2. Diffraction pattern of 18%Ni/γ-Al_2O_3 nanocomposite and theoretical diffraction patterns of Ni and NiO phases: (*1*) Ni phase; (*2*) NiO phase.

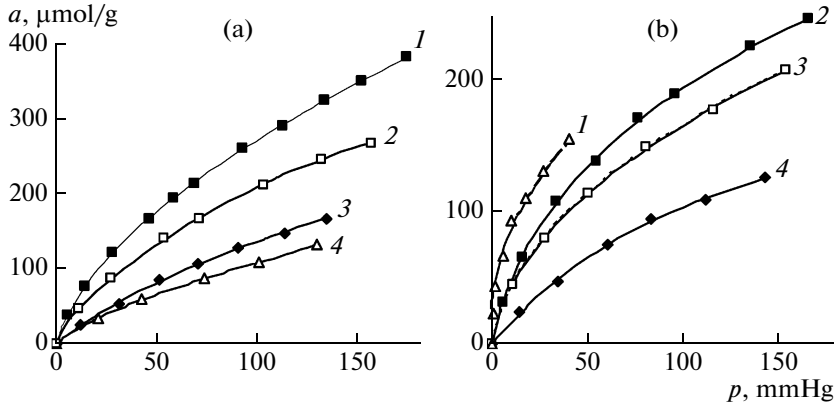

Fig. 3. Adsorption isotherms at 100°C: (a) benzene on (*1*) $Al_2O_3^*$ and (*2*) 12% Ni/Al_2O_3; *n*-hexane on (*3*) $Al_2O_3^*$ and (*4*) 12% Ni/Al_2O_3. (b) (*1*) diethyl ether, (*2*) benzene, (*3*) chloroform, and (*4*) *n*-hexane on 18% Ni/Al_2O_3.

The deposition of nickel onto a surface of γ-Al_2O_3 reduces its specific surface area. The radii of pores did not change significantly. According to IUPAC and the Dubinin classifications of pores [11], these can be considered mesopores (with diameters of 2 to 50 nm).

Adsorption Heats of Test Adsorbates

Dependences of isosteric heats of adsorption Q_{st} were calculated from isotherms of adsorption on γ-$Al_2O_3^*$ and Ni/γ-Al_2O_3 composites.

Q_{st} values and the contributions to them from dispersive (Q_{dis}) and specific (donor-accepting) (Q_{spec}) interactions in areas of low filling ($a = 0.5$ μmol/m^2) during adsorption on γ-$Al_2O_3^*$ and composites are presented in Table 4. The contribution from the energy of specific interaction (Q_{spec}) was determined as the difference between the Q_{st} values of (a) a polar adsorbate and (b) a hypothetical *n*-alkane with the same total polarizing ability.

As can be seen from Table 4, the deposition of Ni on a γ-Al_2O_3 surface raises the heats of adsorption of *n*-alkanes; for polar adsorbates, it increases the contribution from the energy of dispersive interactions to the total energy of adsorption, particularly in the case of 18% Ni/γ-Al_2O_3 composite. The contribution from the energy of specific interactions (Q_{spec}) to the total energy of adsorption of the components changes differently in comparison to γ-$Al_2O_3^*$: it rose considerably for 0.6% Ni/γ-Al_2O_3 composite both in the case of electron-accepting ($CHCl_3$) and electron-donating ($(C_2H_5)_2O$) molecules; for 12% Ni/γ-Al_2O_3 compos-

Table 3. Parameters of the porous structure of γ-$Al_2O_3^*$ and 12% Ni/γ-Al_2O_3 and 18% Ni/γ-Al_2O_3 nanocomposites

Adsorbent	s, m^2/g	E_0, kcal/g	r, nm
γ-$Al_2O_3^*$	101	10.3	1.16
0.6% Ni/γ-Al_2O_3	79	10.4	1.15
12% Ni/γ-Al_2O_3	81	10.1	1.19
18% Ni/γ-Al_2O_3	83	11.0	1.09

ite, it grew in the case of $CHCl_3$ and fell substantially for $(C_2H_5)_2O$, demonstrating the electron-donating (basic) character of a surface of this composite.

For 18% Ni/γ-Al_2O_3 composite, the contribution from the energy of specific interactions (Q_{spec}) diminished for $CHCl_3$, and most of all for $(C_2H_5)_2O$. Diethyl ether was adsorbed on a surface of this composite due mainly to dispersion interactions. The contribution from the energy of specific interactions (Q_{spec}) to the total energy of adsorption in the case of $(C_2H_5)_2O$ was only 6%.

The energy of specific interactions is determined by the electron-donating and electron-accepting properties of adsorbate molecules and the molecules of an adsorbent surface, and can be expressed by the equation [13]:

$$Q_{spec}/AN = K_D + K_A DN/AN, \quad (3)$$

where K_A and K_D denote the electron-accepting and electron-donating energy characteristics of the surface, and AN and DN denote the electron-accepting and electron-donating properties of molecules of the adsorbate.

The electron-donating K_D and electron-accepting K_A characteristics of a γ-$Al_2O_3^*$ surface and composite surfaces, estimated using Eq. (3), are listed in Table 5.

As can be seen from Table 5, the energy characteristics of electron-accepting sites on a surface of 0.6% Ni/γ-Al_2O_3 composite grew rapidly, while those of sites on surfaces of 12% Ni/γ-Al_2O_3 and 18% Ni/γ-Al_2O_3 composites declined rapidly. The characteristics of electron-donating sites change to a lesser degree (they grew on surfaces of 0.6% Ni/γ-Al_2O_3 and 18% Ni/γ-Al_2O_3 composites, and declined on surfaces of 18% Ni/γ-Al_2O_3 composite) relative to γ-$Al_2O_3^*$.

On the basis of these data, we may conclude that the adsorption properties of the studied nanocomposites are determined by the size and chemistry of surface nanoclusters (Ni and NiO nanoclusters for 12% Ni/γ-Al_2O_3 and Ni nanoclusters in the case of 18% Ni/γ-Al_2O_3.

Adsorption Isotherms of Chlorobenzenes

The isotherms of chlorobenzene and *o*-dichlorobenzene adsorption at 125 and 150°C on parent γ-Al_2O_3 and on samples modified with Ni nanoparticles cluster toward the axis of adsorption, indicating that adsorbate–adsorbent interaction is stronger than adsorbate–adsorbate interaction (Fig. 4). At all equilibrium pressures, the adsorption of C_6H_5Cl and *o*-$C_6H_4Cl_2$ on parent Al_2O_3 and modified samples diminishes as the temperature rises; this usually indicates adsorption is of a physical character.

Adsorption of these adsorbates at the same equilibrium pressure was highest on modified samples with low contents of Ni (up to 3%), and lowest on the samples with surfaces fully coated with Ni clusters (6–18 wt %). The deposition of small amounts of nickel had no appreciable effect on the structure and surface chemistry of adsorbent, and thus did not change the adsorption properties of either chlorobenzene. Although, the higher nickel loads (12 and 18%) on γ-Al_2O_3 leads to marked lowering of adsorption isotherms for both chlorobenzenes. This was probably a

Table 4. Values of Q_{st} and contributions from the energy of dispersive (Q_{disp}) and specific (Q_{spec}) interactions, kJ/mol

Adsorbate	γ-$Al_2O_3^*$			0.6% Ni			12% Ni			18% Ni		
	Q_{st}	Q_{disp}	Q_{spec}	Q_{st}	Q_{disp}	Q_{spec}	Q_{st}	Q_{disp}	Q_{spec}	Q_{st}	Q_{disp}	Q_{spec}
n-C_6H_{14}	35	35	0	32	32	0	37	37	0	50	50	0
n-C_7H_{16}	41	41	0	42	42	0	44	44	0	54	54	0
n-C_8H_{18}	47	47	0	52	52	0	51	51	0	57	57	0
C_6H_6	40	30	10	38	24	14	49	31	18	55	47	8
$CHCl_3$	39	23	16	46	12	34	48	23	25	55	43	12
$(C_2H_5)_2O$	47	27	20	54	19	35	33	28	5	49	46	3

result of changes in their surface chemistry upon a reduction of specific surface area or a change in texture, due not only to the amount of deposited nickel but also to the sizes of its nanoclusters.

Heats of Adsorption of Chlorobenzenes

Table 6 presents the filling dependences of isosteric heats of adsorption (Q_{st}), calculated from adsorption isotherms measured at different temperatures. Upon filling the of γ-Al_2O_3 and composites, the heats of adsorption of *o*-dichlorobenzene are more than twice as high as the heats of adsorption of C_6H_5Cl.

At low surface filling ($a = 0.5$ μmol/m^2), the highest values of adsorption heats for both C_6H_5Cl, and *o*-$C_6H_4Cl_2$ are observed for the composite with the lowest Ni content, 0.6% Ni/γ-Al_2O_3. Heats of adsorption fall as the Ni content in composites rises. At very low degrees of filling, adsorption occurs primarily on the most active surface sites; upon filling, it occurs on less active sites, lowering the heats of adsorption. Such sites on γ-Al_2O_3 surfaces are Brønsted and Lewis acid sites with different forces. Lewis sites are less fully coordinated aluminum atoms that form during dehydration; weak Brønsted sites are of the Lewis type with adsorbed water [14]. The active sites of our modified samples were Ni and NiO nanoclusters.

The heat of adsorption can be used to estimate the type of adsorption: physical or chemical. The values of the heat of physical adsorption are usually in the range of 30–70 kJ/mol, while values of the heat of chemical adsorption lie in the range of 80–400 kJ/mol [15]. As can be seen from Table 6, adsorption heats of C_6H_5Cl on parent γ-Al_2O_3 and Ni/γ-Al_2O_3 composites are slightly higher than the values typical of physical adsorption, while the adsorption heat of *o*-$C_6H_4Cl_2$ lies in the range of values typical of chemical adsorption. This indicates that C_6H_5Cl is physically adsorbed, forming donor-accepting complexes with active sites on surface of these adsorbents, while *o*-$C_6H_4Cl_2$ is chemically adsorbed on the most active sites, forming valence bonds with surface.

Table 5. Electron-accepting (K_A) and electron-donating (K_D) surface characteristics (kJ/mol)

Adsorbent	K_A	K_D
γ-$Al_2O_3^*$	0.21	0.69
0.6%/γ-Al_2O_3	0.36	1.46
12% Ni/γ-Al_2O_3	0.01	1.07
18% Ni/γ-Al_2O_3	0.02	0.51

Free Energy and the Entropy of Adsorption

Differential molar changes in the free energy of adsorption ((ΔF)) were calculated for C_6H_5Cl and *o*-$C_6H_4Cl_2$ from the adsorption isotherms at 125°C and $a = 0.5$ μmol/m^2 on γ-$Al_2O_3^*$ and composites using the equation

$$\Delta F = RT \ln(p/p_s), \quad (4)$$

where p is the equilibrium pressure of the adsorbate vapor, p_s is the pressure of the adsorbate's saturated vapor at a given temperature, T is temperature; and differential molar changes of adsorption entropy (ΔS) are calculated using the equation:

$$\Delta S = -(Q_{st} + \Delta F)/T, \quad (5)$$

where Q_{st} is the isosteric adsorption heat at $a = 0.5$ μmol/m^2; ΔF is the differential molar change of

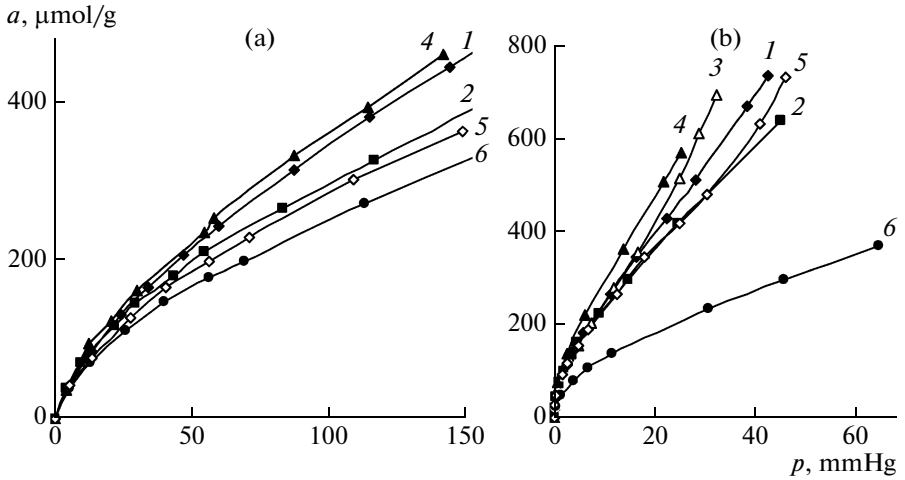

Fig. 4. Adsorption isotherms of (a) C_6H_5Cl and (b) $C_6H_4Cl_2$ on parent ((*1*) γ-Al_2O_3*) and on modified ((*2*) 0.6, (*3*) 1.5, (*4*) 3, (*5*) 12, (*6*) 18% Ni) γ-Al_2O_3 samples at 125°C.

Table 6. Dependency of Q_{st}, kJ/mol of C_6H_5Cl and o-$C_6H_4Cl_2$ on adsorption, (a, μmol/g)

a	Al_2O_3 par	$Al_2O_3^*$	0.6% Ni	1.5% Ni	3% Ni	12% Ni
			C_6H_5Cl			
50	67	58	70	59	58	53
60	66	58	69	58	57	54
70	64	59	68	57	57	53
80	62	59	66	55	57	56
90	61	59	65	54	57	56
100	60	58	63	53	58	57
110	59	58	62	52	58	56
140	56	56	57	50	59	56
150	56	56	56	49	60	55
160	55	55	55	48	60	54
170	54	54	54	48	60	54
180	54	53	54	47	60	53
			o-$C_6H_4Cl_2$			
50	132	130	149	135	126	128
100	108	107	112	98	111	105
150	97	95	97	89	99	98
200	91	89	89	86	84	94
250	85	84	85	85	84	90
300	83	81	82	85	83	87
350	80	78	79	85	81	85
400	78	75	76	86	79	82
450	77	71	74	88	79	81

free adsorption energy of adsorption, and T is temperature.

Table 7 presents the obtained values and the ΔS_{theor} values calculated using the equation derived by molecular statistics in [16],

$$\Delta S_{theor} = R\ln(MT)^{1/2} + 56.95 + R, \quad (6)$$

where M is the molecular mass of the adsorbate and T is temperature.

In areas of low surface filling, the adsorbate forms an ideal two-dimensional gas on the surface of the adsorbent; the drop in the entropy of adsorption (ΔS) is due to the loss of only one degree of freedom.

As can be seen from Table 7, the ΔS_{exp} values are slightly higher than the ΔS_{theor} values in the case of adsorption of C_6H_5Cl on γ-$Al_2O_3^*$ and composites, and for o-$C_6H_4Cl_2$ the ΔS_{exp} values are ~3 times higher than those of ΔS_{theor}. In this case, any molecular motion (except for vibrational motion) would be difficult. Adsorption remains localized on the most active sites.

This also indicates that C_6H_5Cl is physically adsorbed, while o-$C_6H_4Cl_2$ is chemically adsorbed on especially active sites.

In heterogeneous catalysis, the chemosorption of reagents is the most important stage and ensures the progress of the reaction. Reagents are activated during adsorption, and the higher the potential of an active site, the higher the adsorption heat and the degree of activation of reagent molecules.

CONCLUSIONS

From our analysis of the experimental data, we can see that benzene and chlorobenzene are physically sorbed, while o-dichlorobenzene is chemically sorbed under the considered conditions.

The highest values for the adsorption heats of chlorobenzene and o-dichlorobenzene were observed on 0.6% Ni/γ-Al_2O_3. This was probably due to the size effect upon increasing the concentrations of surface metal atoms in different coordination environments [5].

ACKNOWLEDGMENTS

The authors are grateful to E.S. Lokteva, E.A. Golubina, and A.A. Erokhin for technical support during samples synthesis.

Table 7. Differential molar changes in free energy of adsorption (ΔF, kJ/mol) and differential changes in entropy (ΔS, J/(mol K)) of adsorption at $a = 0.5$ μmol/m^2 on γ-$Al_2O_3^*$ and nanocomposites

Adsorbate	$Al_2O_3^*$		0.6%Ni/Al_2O_3		12%Ni/Al_2O_3		18%Ni/Al_2O_3		ΔS_{theor}
	$-\Delta F$	$-\Delta S$	$-\Delta F$	$-\Delta S$	$-\Delta F$	$-\Delta S$	$-\Delta F$	$-\Delta S$	
C_6H_5Cl	16	105	17	134	16	93	16	126	92
o-$C_6H_4Cl_2$	25	264	25	312	24	262	24	60	93

This work was supported by the Russian Foundation for Basic Research, project nos. 10-03-00999, 12-03-00595, and 11-03-01011.

REFERENCES

1. V. I. Bukhtiyarov and M. G. Slin'ko, Russ. Chem. Rev. **70**, 147 (2001).
2. M. Haruta, T. Kobayashi, H. Sano, and N. Yamada, Chem. Lett. **16**, 405 (1987).
3. M. Haruta, Chem. Record **3**, 75 (2003).
4. A. L. Buchachenko, Russ. Chem. Rev. **72**, 375 (2003).
5. S. A. Nikolaev, Candidate's Dissertation in Chemistry (Moscow State Univ., Moscow, 2006).
6. M. D. Navalikhina and O. V. Krylov, Russ. Chem. Rev. **64**, 586 (1998).
7. S. A. Kachevskii, E. V. Golubina, E. S. Lokteva, and V. V. Lunin, Russ. J. Phys. Chem. A **81**, 866 (2007).
8. V. Gutmann, Electrochim. Acta **21**, 661 (1976).
9. *Experimental Methods in Adsorption and Chromatography*, Ed. by Yu. S. Nikitin and R. S. Petrova (Mosk. Gos. Univ., Moscow, 1990), p. 313 [in Russian].
10. A. V. Kiselev, N. V. Kovaleva, and Y. S. Nikitin, J. Chromatogr. **58**, 19 (1971).
11. M. M. Dubinin, *Adsorption and Porosity* (Akad. Khimzashchity, Moscow, 1972), p. 123 [in Russian].
12. G. M. Plavnik and M. M. Dubinin, Russ. Chem. Bull. **15**, 597 (1966).
13. J. B. Donnet and S. Park, Carbon **29**, 955 (1991).
14. A. V. Kiselev and V. I. Lygin, *Infrared Spectra of Surface Compounds* (Nauka, Moscow, 1972), p. 459 [in Russian].
15. A. P. Karnaukhov, *Adsorption. Texture of Disperse and Porous Materials* (Nauka, Novosibirsk, 1999), p. 469 [in Russian].
16. A. A. Lopatkin, Zh. Ross. Khim. Obshch. Mendeleeva **40** (2), 5 (1996).

Translated by E. Chernova